

Needle Tracking Algorithm

Chen Wang, Kai Wang, Xinyi He, Siyue Zhou, Zhaoshuo Li

Abstract—Lumbar puncture is used as a technique to diagnose central nervous system disorders with a needle. Currently, to provide visual guidance through ultrasound, the needle needs to be tracked accurately. This project proposes a tracking algorithm to track the needle position with a small laser projector at the end of the needle. The feasibility test is done with a laser pointer tracked by a pair of stereo camera. The result has shown that sub-millimeter accuracy cannot be achieved with the current approach.

I. INTRODUCTION

Lumbar puncture is used as a technique to diagnose central nervous system disorders by extracting cerebrospinal fluid. Currently, the processes is performed blindly, leading to a 23.3% failure rate [1]. Thus, a single element ultrasound has been developed to assist the process by providing real-time imaging information [2]. It requires the puncture needle needs to be accurately tracked. Therefore, this project proposes an algorithm to track the needle position with a small laser projector at the end of the needle. With the projector projecting a known pattern on the ceiling, in theory the needle position and orientation can be found by utilizing the laser intrinsic parameter and the location of the pattern. Since the motion of the hand is amplified due to the distance between the laser and ceiling, we hope to achieve sub-millimeter accuracy with a much cheaper and viable solution compared to commercial products.

II. METHODOLOGY

We calibrate the laser pointer to obtain the ratio of the geometry of the pattern over focal length assuming a pinhole camera model. Through image processing, we extract feature points in the pattern and find the correspondences. With calibrated stereo cameras (known intrinsic and extrinsic), the 3D location of the pattern can be found. We can then recover the pose and position of laser pointer by solving the perspective-n-pair (PnP) problem [3].

A. Camera Calibration

To recover the 3D location, we must find the intrinsic and extrinsic of the stereo pair. Also, the cameras will introduce the radial and tangential distortion to images, which will need to be corrected.

Due to radial distortion, straight lines will appear curved. Its effect is more as we move away from the center of the image. And this distortion is represented as follows:

$$\begin{aligned} x_{distorted} &= x(1 + k_1r^2 + k_2r^4 + k_3r^6) \\ y_{distorted} &= y(1 + k_1r^2 + k_2r^4 + k_3r^6) \end{aligned}$$

Another distortion is the tangential distortion which occurs because image taking lense is not aligned perfectly parallel to

the imaging plane. So some areas in image may look nearer than expected. The equations are represented as below:

$$\begin{aligned} x_{distorted} &= x + [2p_1xy + p_2(r^2 + 2x^2)] \\ y_{distorted} &= y + [p_1(r^2 + 2y^2) + 2p_2xy] \end{aligned}$$

The calibration is done by using a checkerboard with square side to be 40mm. The extrinsic error is 0.4198mm in translation and the re-projection error is 0.8px. The camera parameters such as brightness, contrast and saturation are also tuned (0.8, 0.8, 0.2 respectively) for the best imaging quality.

B. Laser Pointer Calibration

Solving the location and orientation of the laser pointer is essentially a PnP problem, except that we have a laser pointer. Since the PnP problem is only dependent on the ratio between focal length and pattern size assuming a pinhole camera model, we only need to obtain the ratio when calibrating for the intrinsics. Moreover, during calibration the laser position is not known exactly, the difference in size of the projected pattern is utilized to calculate the ratio, and the mathematical derivation is shown below.

According to similar triangles, we can derive the equations

$$\frac{a}{d} = \frac{b}{e} = \frac{c}{f} \quad (1)$$

$$\frac{a}{d} = \frac{b-c}{e-f} \quad (2)$$

Thus, we can calculate the ratio of a and d without knowing a and d . Here, a is the focal length and d is the distance between feature points and center point.

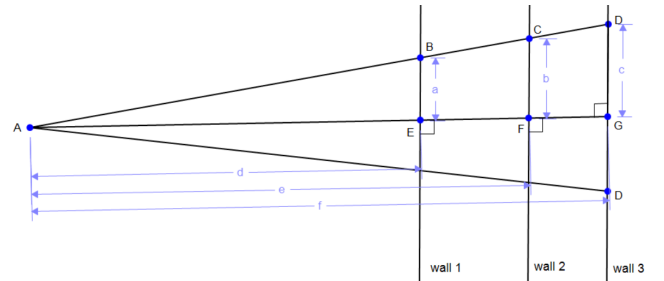


Fig. 1. Point A is the light source. Point E, F, G are the centre point of the projected image on wall 1, wall 2, and wall 3. Point B, C, D are the projected feature point on wall 1, wall 2, and wall 3.

We attached the laser pointer to an UR5 (Universal Robot). By setting the Y axis of the robot perpendicular to the wall, we move the UR5 along the axis by 120 mm each step. The length between midpoint and feature points are measured

at each step. The slope of the fitted trend line is the ratio that we want to obtain. The resulted calibration returns an average of R^2 is 0.965625. The Figure 2 shows the selected eight feature points we calibrated. They are chosen to be the corners of the pattern to be easily detected.



Fig. 2. Selected feature points (green) and projected pattern (red).

C. Feature Point Detection

To find the feature points, the input is processed by the following steps:

- Diffusion filter: Since the image input has bright part and dark region, the noise is anisotropic around the edge, the diffusion filter is used to remove background noise and preserve the edge.
- Brightest pixel in gray scale: The input image is then converted to gray scale and the brightest pixel is take as the centre of the pattern.
- HSV filter: A mask of the pattern is created since the color is known to be red, and a bit-wise AND operation is done on the gray image to only keep the desired pattern.
- Binarization and Morphological Thinning: The masked gray image is binarized based on the average intensity of the contour, and the image is further thinned to a skeleton such that corners of line intersection can be found.
- Harris corner[4]: Find candidate points.

D. Point corresponding

To find the corresponding known feature points from all feature point candidates, we first find the shift, scale and orientation to best match the point sets. The shift between the two point sets can be found by center-center distance. Then, the scale between the known point set and the candidate point set is calculated by the ratio of the maximum deviation from centre point, *i.e.*

$$scale = \frac{||mean_{p-p_c} + 1.5 \cdot std_{p-p_c}||, p \in CandidateSet}{argmax||p - p_c||, p \in KnownSet} \quad (3)$$

Then, the orientation of the pattern is estimated by using a minimum ellipse to enclose all candidates and find the direction of principle axis. However, the result is only from -90° to 90° . A potential solution, though has not been implemented, is to rotate the known point by a certain angle

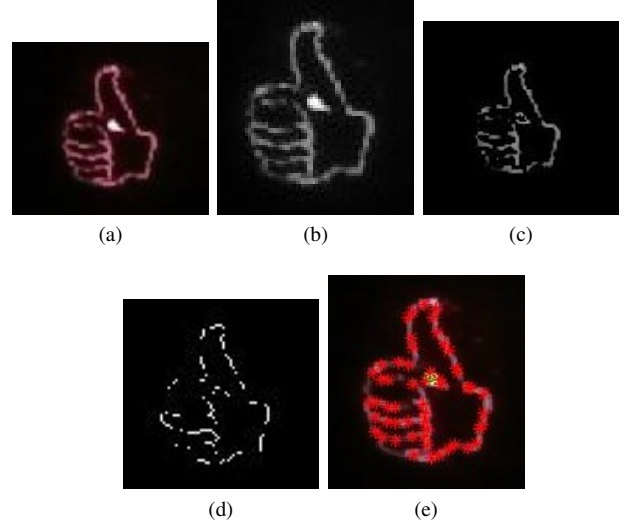


Fig. 3. Cropped images to demonstrate the image processing, (a) Diffusion Filtered, (b) Gray Scale, (c) HSV Filtered (d) Morphological Thinned (e) Harris Corner

and an angle 180° from the calculated value, and choose the one gives minimum error.

Afterwards, the iterative closest point [5] is used to find the correspondence. First, the closest point in the candidate set to the points known set is found. For the distances of point pairs lie within a threshold, the point pairs will be marked as inlier and 2D-2D rigid transformation will be calculated using [6]. With the transformation, the closest points in candidate set to known set will be marked as found feature and returned (shown in Figure 4).

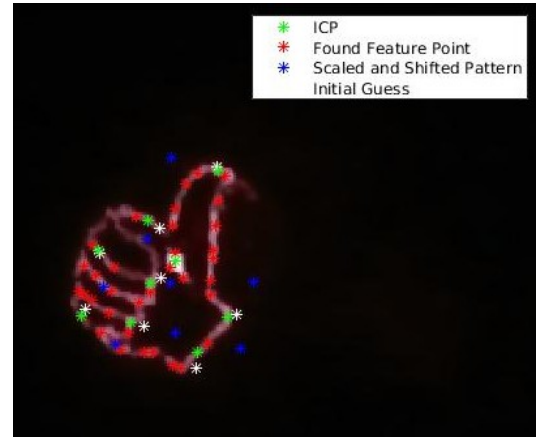


Fig. 4. Point Correspondence. Green: Closest points in candidates. Red: Candidates. Blue: Scaled and shifted template. White: Initial guess with rotation applied.

E. Perspective Transformation

To perform the perspective transformation, we first need the 3D location of the feature points. This is done through triangulation by solving the epipolar equations. The reconstructed point cloud is shown in Figure 5.

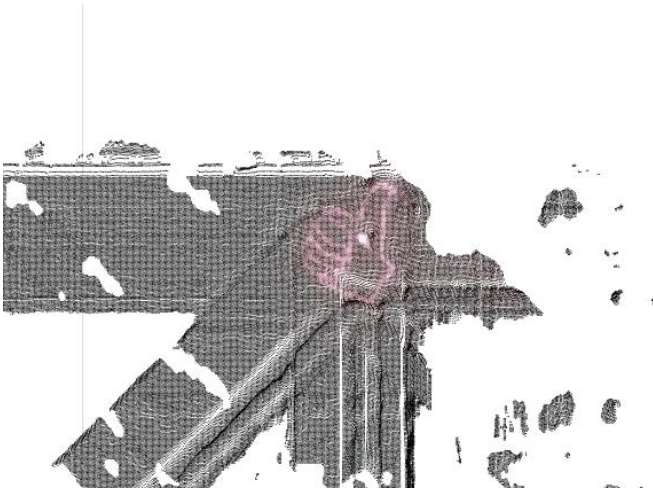


Fig. 5. 3D reconstructed point cloud.

Our algorithm further detects outliers by two criteria. First, since corresponding point pairs have the same height in rectified images, if any matched points found in the left and right images do not have a y-axis error less than 3 pixels (original image size 1280×960 pixels), we define the point pairs as outliers. Moreover, we know that the camera is nearly parallel to the projected plane (ground or ceiling), the reconstructed 3D points should have the same depth. Therefore, any points that have a depth value deviates from the mean depth of all detected points by one standard deviation, they are marked as outliers. With the 3D locations, the PnP problem is solved with a minimum of 4 points. If fewer than 4 points are found in the image, the algorithm will return the image pair as a failure case.

III. RESULT AND CONCLUSION

We attached the laser pointer to UR5 and moved it along its X and Y axis in an increment of $50mm$. The algorithm fails to detect more than 4 points in the detected feature set in 6 out of 16 input images due to strong reflection and shadowing issue (see Figure 6 b). The position is also tabulated below. As shown, the result is very noisy and has significant movement in Z axis, which should have been constant. The algorithm fails to recover the pose of the laser pointer with significant noise.

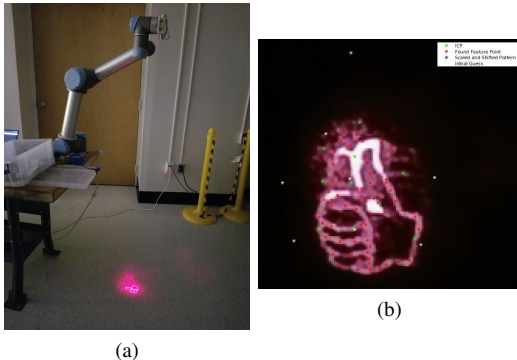


Fig. 6. (a)Experimental Setup. (b) Failure case.

TABLE I
COORDINATES OF UR5 AND RECOVERED LASER (UNIT:MM)

UR5 X	UR5 Y	UR5 Z	Laser X	Laser Y	Laser Z
526.25	199.96	760.17	245.7361	-327.1918	-298.1919
526.25	149.96	760.17	151.5667	-136.0869	-519.4902
526.25	100.00	760.17	595.9162	-224.1241	-521.3240
526.25	50.00	760.17	NaN	NaN	NaN
526.25	0.00	760.17	NaN	NaN	NaN
526.25	-50.00	760.17	NaN	NaN	NaN
526.25	-100.00	760.17	115.1726	-591.7168	-595.0351
475.96	49.98	760.17	NaN	NaN	NaN
426	49.98	760.1	-377.6306	538.9373	-245.6026
376	49.98	760.1	483.2470	374.9338	-510.1105
326	49.98	760.1	-269.6036	-135.1897	-616.3761
276	49.98	760.1	NaN	NaN	NaN

Then UR5 is rotated around the Z-axis for 30 degrees each step. The result is tabulated below. Even though the rotation follows the trend of rotation, the values do not match.

TABLE II
ROTATION OF UR5 AND RECOVERED LASER (UNIT:DEGREE)

UR5 RX	UR5 RY	UR5 RZ	Laser RX	Laser RY	Laser RZ
-92.61	1.68	-50	-2.5874	10.0970	14.6784
-92.63	1.68	-80.05	4.8075	39.4005	71.3388
-92.63	1.68	-110.05	NaN	NaN	NaN
-92.63	1.68	-140.05	-0.5063	-16.8142	-57.2525
-92.63	1.68	-20	-7.9495	23.9832	-37.2224

Another simulation study is done to introduce noise in 3D points with a random error up to $1mm$ given a projected pattern of size $50mm$, and the laser location and orientation error is found to be $8.3mm$. Thus, the conclusion is as following. Firstly, the laser pointer calibration is inaccurate with around $5mm$ error during manual measurement. Secondly, the recovery of the 3D location of the feature points has a mean error $14.13mm$, stddev $23.17mm$. The system can be significantly improved if the projected pattern is in the form of AR marker, whose pose and orientation is already encoded in the shape. Also, if the laser intrinsics is accurately known, the result will be improved.

REFERENCES

- [1] C. Armon and R. W. Evans, "Addendum to assessment: Prevention of post-lumbar puncture headaches report of the therapeutics and technology assessment subcommittee of the american academy of neurology," *Neurology*, vol. 65, no. 4, pp. 510-512, 2005.
- [2] H. K. Zhang, Y. Kim, M. Lin, M. Paredes, K. Kannan, A. Moghekar, N. J. Durr, and E. M. Boctor, "Toward dynamic lumbar puncture guidance using needle-based single-element ultrasound imaging," *Journal of Medical Imaging*, vol. 5, no. 2, p. 021224, 2018.
- [3] P. H. Torr and A. Zisserman, "Mlesac: A new robust estimator with application to estimating image geometry," *Computer vision and image understanding*, vol. 78, no. 1, pp. 138-156, 2000.
- [4] C. Harris and M. Stephens, "A combined corner and edge detector," in *Alvey vision conference*, vol. 15, no. 50. Citeseer, 1988, pp. 10-5244.
- [5] P. J. Besl and N. D. McKay, "Method for registration of 3-d shapes," in *Sensor Fusion IV: Control Paradigms and Data Structures*, vol. 1611. International Society for Optics and Photonics, 1992, pp. 586-607.
- [6] K. S. Arun, T. S. Huang, and S. D. Blostein, "Least-squares fitting of two 3-d point sets," *IEEE Transactions on Pattern Analysis & Machine Intelligence*, no. 5, pp. 698-700, 1987.